

1 **PGSbuilder: An end-to-end platform for human genome association analysis**  
2 **and polygenic risk score predictions**

3  
4 Ko-Han Lee<sup>1,†</sup>, Yi-Lun Lee<sup>1,†</sup>, Tsung-Ting Hsieh<sup>1,†</sup>, Yu-Chuan Chang<sup>1,†</sup>, Su-Shia Wang<sup>1</sup>, Geng-  
5 Zhi Fann<sup>1</sup>, Wei-Che Lin<sup>1</sup>, Hung-Ching Chang<sup>1</sup>, Ting-Fu Chen<sup>1</sup>, Peng-Husan Li<sup>1</sup>, Ya-Ling Kuo<sup>1</sup>,  
6 Pei-Lung Chen<sup>2,3,4,5</sup>, Hsueh-Fen Juan<sup>1,6,7</sup>, Huai-Kuang Tsai<sup>1,8</sup>, Chien-Yu Chen<sup>1,7,9,\*</sup>, Jia-Hsin  
7 Huang<sup>1,\*</sup>

8  
9 <sup>1</sup>Taiwan AI Labs & Foundation, Taipei 10351, Taiwan  
10 <sup>2</sup>Graduate Institute of Medical Genomics and Proteomics, National Taiwan University College of  
11 Medicine, Taipei 10617, Taiwan

12 <sup>3</sup>Department of Medical Genetics, National Taiwan University Hospital, Taipei 10617, Taiwan  
13 <sup>4</sup> Genome and Systems Biology Degree Program, National Taiwan University and Academia  
14 Sinica, Taipei 11529, Taiwan

15 <sup>5</sup>Graduate Institute of Clinical Medicine, National Taiwan University College of Medicine,  
16 Taipei 10051, Taiwan

17 <sup>6</sup>Department of Life Science, National Taiwan University, Taipei 10617, Taiwan

18 <sup>7</sup>Center for Computational and Systems Biology, National Taiwan University, Taipei 10617,  
19 Taiwan

20 <sup>8</sup>Institute of Information Science, Academia Sinica, Taipei, 11529, Taiwan

21 <sup>9</sup>Department of Biomechatronics Engineering, National Taiwan University, Taipei 10617,  
22 Taiwan

23  
24 <sup>†</sup>Ko-Han Lee, Tsung-Ting Hsieh, Yi-Lun Lee, and Yu-Chuan Chang contributed equally to this  
25 work.

26  
27 <sup>\*</sup>Correspondence: Chien-Yu Chen (chiencyuchen@ntu.edu.tw); Jia-Hsin Huang  
28 (jiahsin.huang@ailabs.tw)

29  
30

31 **Abstract**

32

33 Understanding the genetic basis of human complex diseases is increasingly important in the  
34 development of precision medicine. Over the last decade, genome-wide association studies  
35 (GWAS) have become a key technique for detecting associations between common diseases and  
36 single nucleotide polymorphisms (SNPs) present in a cohort of individuals. Alternatively, the  
37 polygenic risk score (PRS), which often applies results from GWAS summary statistics, is  
38 calculated for the estimation of genetic propensity to a trait at the individual level. Despite many  
39 GWAS and PRS tools being available to analyze a large volume of genotype data, most  
40 clinicians and medical researchers are often not familiar with the bioinformatics tools and lack  
41 access to a high-performance computing cluster resource. To fill this gap, we provide a publicly  
42 available web server, PGSbuilder, for the GWAS and PRS analysis of human genomes with  
43 variant annotations. The user-friendly and intuitive PGSbuilder web server is developed to  
44 facilitate the discovery of the genetic variants associated with complex traits and diseases for  
45 medical professionals with limited computational skills. For GWAS analysis, PGSbuilder  
46 provides the most renowned analysis tool PLINK 2.0 package. For PRS, PGSbuilder provides six  
47 different PRS methods including Clumping and Thresholding, Lassosum, LDpred2, GenEpi,  
48 PRS-CS, and PRSice2. Furthermore, PGSbuilder provides an intuitive user interface to examine  
49 the annotated functional effects of variants from known biomedical databases and relevant  
50 literature using advanced natural language processing approaches. In conclusion, PGSbuilder  
51 offers a reliable platform to aid researchers in advancing the public perception of genomic risk  
52 and precision medicine for human disease genetics. PGSbuilder is freely accessible at  
53 <http://pgsb.tw23.org>.

54

55

56 **Keywords**

57 GWAS; PRS; SNP; Genotyping; Genetic variant

58

59

60

61

## 62 **Introduction**

63 An ultimate goal of human genetics is to understand the genetic basis of human diseases,  
64 diagnosis, and management. Results from a large amount of genome-wide association studies  
65 (GWAS) have vastly demonstrated that many single nucleotide polymorphisms (SNP) genetic  
66 variants are associated with various complex traits<sup>1</sup>. In early 2023, more than 6,300 studies have  
67 conducted to map over 496,000 associations between human SNPs and diseases/traits in the  
68 GWAS catalog<sup>2</sup>. In the past two decades, the successes of GWAS not only drive the discovery of  
69 deleterious mutations linked to certain disease phenotypes but also imply a general pattern of  
70 polygenicity of common diseases<sup>3,4</sup>. Many common diseases that conform to polygenic  
71 inheritance are underpinned by multiple genetic variants with small or moderate effects<sup>5</sup>. After  
72 the realization of a large proportion of the variance in genetic liability to common diseases,  
73 utilization of causative risk alleles based on the GWAS discoveries for disease risk prediction  
74 has become the potential to stratify patients for precision prevention<sup>6,7</sup>.

75

76 Polygenic risk score (also known as polygenic scores; PRS) is an important methodology to  
77 leverage the genetic contribution of an individual's genotype to measure the genetic liability to  
78 complex traits or diseases<sup>8,9</sup>. Clumping and thresholding (C+T)<sup>10</sup> is the primary PRS method  
79 based on the summary statistics from GWAS by pruning SNPs through a process of Linkage  
80 Disequilibrium (LD) clumping and selecting a *P*-value threshold. Still, it has limitations in the  
81 predictive performance without considering other genetic factors. Currently, several PRS  
82 methods based on the summary statistics apply a different selection of the prior distribution on  
83 the effect sizes of the SNPs under the Bayesian framework. For example, LDpred<sup>11</sup> and  
84 LDpred2<sup>12</sup> improve the prediction performance by enhancing LD modeling based on the  
85 normality assumption. PRS-CS<sup>13</sup> introduces a different concept to provide a continuous  
86 shrinkage (CS) prior to accommodate diverse underlying genetic architectures. Alternatively,  
87 SBayesR<sup>14</sup> and SDPR<sup>15</sup> assume a different mixture of normal distributions on the individual-  
88 level data as input for adaptive modeling of SNP effect size. Lassosum<sup>16</sup> implements a penalized  
89 regression approach with a Lasso-type penalty. Empirical evidence from benchmark experiments  
90 shows that not a single method clearly outperforms all other methods in the prediction accuracy  
91 for all the simulated data and disease traits<sup>12-14,17</sup>. Nevertheless, each different PRS method can

92 potentially improve the development of PRS construction with specific optimization procedures.  
93 Recent studies have demonstrated that the comparison of many PRS methods could facilitate the  
94 future implementation of PRS in clinical settings<sup>18,19</sup>. Although a few practical guidelines have  
95 introduced how best to perform PRS analyses<sup>20-22</sup>, a steep learning curve of implementing those  
96 PRS packages and the computing resources required by some tools are impractical for doctors  
97 and clinical professionals.

98

99 As the popularity of PRS increases, over 400 publications report more than 3,200 polygenic  
100 scores in the Polygenic Score Catalog (<https://www.PGSCatalog.org>)<sup>23</sup>. However, those PRS  
101 studies were predominantly conducted on individuals of European descent<sup>24</sup>. Due to the poor  
102 transferability of PRS across populations<sup>25,26</sup>, one critical step toward effectiveness in PRS  
103 accuracy is to conduct PRS development for the diversity of participants from different  
104 ancestries. Along with the cost of a single genetic test per individual plummeting to less than  
105 US\$50, it becomes feasible to acquire a sufficient cohort size for PRS from the population with  
106 underrepresented ancestries by the medical institutes in different countries. In addition, the  
107 current consensus about the refinement of PRS should include other informative clinical factors  
108 based on their healthy records. To facilitate genetic analysis and PRS development, a  
109 sophisticated analysis platform could enable the construction of PRS in clinical research  
110 efficiently. For example, impute.me is a recently developed web tool to provide basic PRS  
111 estimation using a single method of LDpred to predict individual polygenic risks<sup>27</sup>. To increase  
112 the clinical practice of PRS, a comprehensive comparison of different PRS methods could  
113 leverage the extent of predictive values into a better understanding of the genetic liability for  
114 disease traits.

115

116 In this study, we present PGSbuilder which is an integrated cloud-based platform to analyze  
117 human genotype data. PGSbuilder provides a one-stop service to conduct both GWAS and PRS  
118 analyses and interactively visualize the analysis results. In PGSbuilder, users can run six  
119 different PRS methods as well as the PRS models with clinical factors to compare their  
120 performances concurrently. To the best of our knowledge, no other existing web server offers the  
121 possibility to compare multiple PRS models. Further, the interpretation of PRS is needed to  
122 apply the scores into biological explanations and clinical use. Notably, PGSbuilder also

123 integrates the variant annotation automatically for the candidate SNPs from GWAS and PRS  
124 analyses using Ensembl Variant Effect Predictor (VEP)<sup>28</sup> and biomedical literature mining from  
125 pubmedKB<sup>29</sup>. In addition, our web interface allows easy access to link all genetic analysis results  
126 and candidate SNP information with interactive displays. Finally, users can download all the  
127 analysis output files for further exploration.

128

129

## 130 **Materials and Methods**

### 131 **Data privacy and security**

132 Because genetic data will be uploaded to our server, a wide array of security measures are in  
133 force to ensure data privacy and security. Our local server has ISO 27001 certification for  
134 implementing an information security management system (ISMS). In addition, our server is  
135 designed based on the express MVC (Model-View-Controller) framework that encapsulates our  
136 features surrounded by powerful security layers. All interactions with the server are protected  
137 and secured with HTTPS. Any input data is deleted from our server once the analysis is  
138 completed. With the encryption by a firm one-time password, all analyzed results can only be  
139 accessed by the data uploader via an encrypted connection, within a 14 days timeframe.

140

### 141 **GWAS**

142 To conduct quality control (QC) procedures and following genome-wide association studies  
143 (GWAS), we utilize PLINK 2.0, a comprehensive genome association analysis tool for  
144 population genetics<sup>30</sup>. There are three major steps for QC and two for GWAS. QC consists of  
145 variant filtering, individual filtering, and population stratification while GWAS analysis consists  
146 of principal component analysis (PCA) and association test.

147

148 First, unqualified SNPs are filtered out according to the minor allele frequency, Hardy-Weinberg  
149 equilibrium, and missingness. Secondly, individuals with the high missing rate of SNPs, large  
150 deviation of heterozygosity rate, and high kinship coefficient<sup>31</sup> are also removed. Finally, to  
151 exclude individuals with different populations, population stratification is conducted against the  
152 population in HapMap 3<sup>32</sup>. Most of the QC criteria and recommended thresholds are referred to  
153 Marees et al<sup>33</sup>.

154

155 For the GWAS analysis, the top 10 principal components extracted from PCA are used to correct  
156 the genetic difference between in-group individuals<sup>34</sup>. Of note, the population stratification  
157 during the QC analysis is also conducted via PCA to remove outliers at the level of population,  
158 such as Asians, Africans, or Europeans. Next, the principal components and other provided  
159 covariates are included to correct the genetic effect during association tests. Only the effect size  
160 of autosomal SNPs is calculated using the “glm” function of PLINK 2.0<sup>30,35</sup>.

161

## 162 PRS methods

163 In PGSbuilder, the input dataset is separated into the base, target, and test sets, respectively.  
164 First, QC is applied on both base and target sets, and then GWAS is only performed on the base  
165 set to get the summary statistics. Combining the summary statistics with the target set which is  
166 used for the calculation of linkage disequilibrium (LD) and the selection of hyperparameters,  
167 PGSbuilder performs PRS analysis to build models based on different methods. This pipeline of  
168 PRS analysis is referred to Choi et al<sup>21</sup>. There are six PRS methods provided in PGSbuilder,  
169 including clumping and thresholding, PRSice2, LDpred2, Lassosum, PRS-CS, and GenEpi. Five  
170 methods, except GenEpi, are selected to produce PRS prediction from the external summary  
171 statistics without individual genetic data. On the other hand, GenEpi method is included due to  
172 its consideration of gene-based epistasis, which is a distinct machine learning-based algorithm to  
173 estimate PRS, for comparison.

174

175 *Clumping and Thresholding:* Clumping and thresholding (C+T) is the classical algorithm that  
176 adjusts the LD using clumping and selects SNPs with *P*-value less than a specified threshold to  
177 calculate the PRS for each individual<sup>10</sup>. In PGSbuilder, SNPs within 250 kb away from the index  
178 SNP and have the R-squared over 0.1 with it are assigned to the clump of the index SNP. Nine  
179 thresholds, including  $10^{-8}$ ,  $10^{-7}$ ,  $10^{-6}$ ,  $10^{-5}$ ,  $10^{-4}$ ,  $10^{-3}$ ,  $10^{-2}$ ,  $10^{-1}$ , and 1, are applied to the clumped  
180 SNPs to build PRS models. Beta scores derived from the summary statistics are set as the effect  
181 size estimates directly. The model with the best performance on the target set is selected as the  
182 final PRS model.

183

184 *PRSice2*: PRSice2 is also a clumping and thresholding-based PRS algorithm with a higher  
185 resolution of thresholds<sup>17</sup>. SNPs with a minor allele frequency lower than 0.01 are filtered out.  
186 Like C+T, beta scores are set as the effect size estimates directly.

187

188 *Lassosum*: Lassosum uses penalized regression to adjust the effect size of SNPs for a PRS  
189 model<sup>16</sup>. The summary statistics provide the SNP-wise correlation with the phenotype and the  
190 initial effect size of SNPs. LD blocks are defined from the subpopulation of the 1000 Genome  
191 database, and the LD matrix is calculated from the target set. Additionally, the target set is used  
192 for the selection of hyperparameters to get the best PRS model.

193

194 *LDpred2*: LDpred2 is a Bayesian PRS predictor by adjusting the effect size of SNPs from the  
195 summary statistics<sup>12</sup>. The target set provides the correlation between SNPs for LD estimation  
196 within 3 centimorgan. In PGSbuilder, for summary statistics having more than 10 SNPs with *P*-  
197 value<10<sup>-8</sup>, we implement the “LDpred2-grid” mode to select the best hyperparameters,  
198 including the proportion of causal variants and the heritability. On the other hand, for those with  
199 less significant SNPs, we implement the “LDpred2-inf” mode, an infinitesimal model.

200

201 *PRS-CS*: PRS-CS is a Bayesian polygenic prediction method that infers the posterior effect size  
202 of SNPs from the summary statistics using continuous shrinkage priors<sup>13</sup>. In PGSbuilder, we use  
203 the 1000 Genome dataset as the reference panel for LD estimation. The global shrinkage  
204 parameter is fixed at 0.2 and other parameters are left as defaults.

205

206 *GenEpi*: GenEpi, a machine learning approach, takes both additive effect and SNP-SNP  
207 interactions into consideration to build a PRS model from the raw genomic data<sup>36</sup>. GenEpi uses  
208 two-stage feature selection to select a single SNP, intragenic interaction, and intergenic  
209 interaction and then applies a regression model to fit the selected features. In PGSbuilder, we  
210 only train the GenEpi model on the base set.

211

## 212 Covariates

213 In GWAS analysis, covariates are used to adjust the genetic effect on the target phenotype.  
214 PGSbuilder performs PCA before GWAS, and the top ten principal components (PCs) are served

215 as covariates. In addition, users can provide a covariate file, and covariates with the variance  
216 inflation factor (VIF) less than 50 or a missing rate over 20% are removed. Finally, the effect  
217 size of each SNP is corrected with PCs and provided covariates during the association test.

218

219 On the other hand, to provide a comprehensive risk assessment for individuals, features other  
220 than genetic factors should be taken into consideration. After building a PRS model, PGSbuilder  
221 combines the PRS score as a genetic factor and user-provided covariates as clinical factors to  
222 build a regression model trained on the target set. Then, PGSbuilder predicts each individual  
223 using this regression model to stratify the risk of the target phenotype.

224

## 225 Variant annotation tools

226 The annotation of significant SNP from GWAS or other genomic analysis is of great importance.  
227 Annotation of variants is vital for the translation of genomic results to the functional level for  
228 further analysis. The Ensembl Variant Effect Predictor (VEP) is an open-source, powerful, and  
229 versatile toolset for the annotation and prioritization of genomic variants for a transcript or even  
230 non-coding region<sup>28</sup>. We select VEP (version 106) because of its broad collection of databases,  
231 scalability, and free open license. In order to display the important variant information to show  
232 first on the web page, PGSbuilder sorts the VEP results by several criteria, including transcript  
233 consensus, mutation consequence, mutation severity, and feature biotype. The complete VEP result  
234 is provided in the downloaded file. In addition, allele frequencies from Taiwan Biobank<sup>37</sup> and  
235 1000 Genome Project are provided in the VEP annotation.

236

237 Moreover, we integrate our literature mining engines, variant2literature<sup>38</sup> and pubmedKB<sup>29</sup>, by  
238 retrieving entity mentions and odds ratio statistics to create a report of textual evidence for each  
239 variant-phenotype pair. The literature report contains an overall summary and single paper  
240 snippets. For the overall summary, we first collect sentences and clinical case sentences where  
241 the target variant and phenotype are both mentioned. We then present the most important  
242 sentences and clinical cases identified by page rank<sup>39</sup>. For single paper snippets, we present the  
243 paragraph describing odds ratio statistics of the target variant and phenotype.

244

245 Example Data

246 *Taiwan Biobank*: Taiwan Biobank (TWB) is a prospective cohort study with genomic data and a  
247 variety of phenotypes collected from Taiwanese population<sup>37</sup>. The TWB cohort contains 27,500  
248 individuals genotyped for 653,288 SNPs on the TWB v1.0 array as well as 68,978 individuals  
249 genotyped for 748,344 SNPs on the TWB v2.0 array.

250

251 *NIA ADC Cohort*: The NIA ADC Cohort consists of individuals evaluated clinically from  
252 National Institute on Aging (NIA)-funded Alzheimer Disease Centers (ADC)<sup>40</sup>. Inclusion criteria  
253 of late-onset Alzheimer's disease are autopsied subjects with age >60 or cases diagnosed with  
254 DSM-IV or Clinical Dementia Rating >1<sup>40</sup>. All the seven ADC datasets downloaded from  
255 NIAGADS (<https://www.niagads.org/datasets>) were merged directly as a joint analysis. In total,  
256 there are 10,256 samples, including 5,334 cases, 3,973 controls, and 949 unknowns, genotyped  
257 for 914,402 SNPs.

258

259

260 **Results**

261 PGSbuilder analysis workflow

262 PGSbuilder is a web-based server to provide end-to-end analysis for genetic cohort data  
263 including GWAS, PRS, and variant annotation. The GWAS analysis aims to figure out the  
264 significant SNPs associated with a specific phenotype while the PRS analysis aims to build a  
265 model for the estimation of the individual risk. After the analysis, SNP-level annotation and  
266 literature exploration using pubmedKB<sup>29</sup> are performed to provide useful insights into causal  
267 variants.

268

269 The GWAS pipeline (Figure 1), which is applied to the whole input dataset, consists of quality  
270 control (QC) and association tests. As for the PRS pipeline (Figure 1), the input dataset is firstly  
271 separated into training and test sets. The training set is undergone QC steps and split into base  
272 and target subsets. The base subset is used to obtain the summary statistics of GWAS, while the  
273 target subset is used to build the PRS models. On the other hand, the option of an external  
274 summary statistics file is available in PGSbuilder. When the external summary statistics file is

275 provided, it replaces the base subset to provide GWAS results and the entire training set serves  
276 as the target subset alternatively. To build a PRS model, most PRS methods combine the  
277 summary statistics providing the initial SNP effect sizes with the linkage disequilibrium (LD)  
278 estimation derived from the target subset. Of note, GenEpi is unavailable for building a PRS  
279 model from the external summary statistics. Finally, to validate the model performance, the  
280 estimated risks of individuals in the test set are independently calculated by the adjusted effect  
281 size.

282

### 283 System implementation

284 We used Kubernetes and docker technology to group our applications including web interfaces,  
285 data processing, GWAS and PRS pipelines, and variant annotation into a service platform. For  
286 the web interface, we adopted React architecture and Node.js for the frontend and backend  
287 respectively. For the analysis, after users upload genotype data, PGSbuilder will create pods for  
288 GWAS and PRS pipelines dynamically and instantly. Significant variants derived from GWAS  
289 and PRS pipelines will be annotated through the VEP and pubmedKB to determine the effect of  
290 variants in the public database and academic literature.

291

292 For the security of private genomic data, users have to sign up via email activation. After login,  
293 two studies including a binary trait (classification model) and a quantitative trait (regression  
294 model) are demonstrated on the analysis page. To create a new study, users have to upload  
295 genotype data in PLINK format and fill in relevant information such as population, genome  
296 build, and prediction method (classification or regression). PGSbuilder provides flexibility for  
297 users to modify some quality control parameters and select multiple PRS methods (Figure 2A). If  
298 the data is successfully uploaded to the PGSbuilder server, the job is added to the analysis queue  
299 and will be processed as soon as possible. Users will receive an email notice to check the state of  
300 jobs on the running page. Once the job is completed, users can download a comprehensive report  
301 for GWAS and PRS results. PGSbuilder also provides an interactive interface to view the result  
302 in detail.

303

304 On the GWAS result page, PCA plot, quantile-quantile plot (Q-Q plot), Manhattan plot, and the  
305 variant table are demonstrated (Figure 2B). PCA is used for the correction of population

306 stratification, and the top 10 principal components (PCs) are selected as covariates for GWAS.  
307 The paired distributions of the top 3 PCs are shown interactively, and users can arbitrarily switch  
308 between three figures through arrow buttons. In addition, each dot represents a sample whose ID  
309 will be displayed via a mouseover event, which can help users discriminate outliers. The Q-Q  
310 plot is provided to evaluate the deviation of observed *P*-values from expected *P*-values under a  
311 uniform distribution. For the Manhattan plot and variant table, we set a suggestive *P*-value  
312 threshold of  $1 \times 10^{-5}$  and a strict *P*-value threshold of  $5 \times 10^{-8}$ . SNPs with a *P*-value smaller than  
313 the threshold are colored in orange and listed in the variant table. The SNPs in the Manhattan  
314 plot and the variant table are interactive. Clicking on an orange point on the Manhattan plot  
315 navigates the variant table to the corresponding SNP with its information, and vice versa.  
316 Besides, users can search for a specific SNP through the search bar. More detailed information of  
317 all SNPs including their *P*-values and annotated information are compressed as a zip file to be  
318 downloaded.

319

320 On the PRS result page, we compare the performance of selected PRS methods. The quantile  
321 plot shows the risk stratification (Figure 2C). For each method, samples in the test set are divided  
322 into 10 quantiles of increasing PRS. Then, in each quantile, the odds ratio is calculated for binary  
323 phenotypes while the mean of values is calculated for quantitative phenotypes. A great difference  
324 between the first and the last group represents a good risk stratification. Of note, all individuals  
325 in the test set serve as the baseline for odds ratio calculation for binary tracts. In the classification  
326 analysis for a binary tract, the receiver operating characteristic (ROC) curve and distribution plot  
327 for each method are demonstrated (Figure 2C). The area under the ROC curve illustrates the  
328 performance and the distribution plots illustrate the prediction distribution for cases against  
329 controls. In the regression analysis for a quantitative tract, Spearman correlations and scatter  
330 plots are shown (Figure 2C). The Spearman correlation is performed to evaluate the performance  
331 and the scatter plot with a regression line illustrates the relationship between phenotypes and  
332 prediction rankings for each method. The tabs of method lists allow users to switch results  
333 between different methods. Users can click one of them to view the corresponding performance  
334 and variant table.

335

336 Furthermore, analysis beyond genetic factors is also available in PGSbuilder. If the covariate file  
337 is provided, covariates will be used to correct the effect size of SNPs during GWAS, and then  
338 serve as clinical factors combined with PRSs to build a regression model for risk prediction. The  
339 performance with or without clinical factors is also demonstrated in the figures for comparison.  
340 The weight of each clinical factor is shown in a table for users to figure out important factors.

341

### 342 Variant annotation panel

343 In order to help interpret GWAS and PRS results, PGSbuilder provides a comprehensive variant  
344 annotation panel for users to explore biological significance. There are often a large number of  
345 SNPs associated with a phenotype. PGSbuilder will automatically sort the important SNPs at the  
346 top of the panel according to several annotation information including transcript consensus,  
347 mutation consequence, mutation severity, and feature biotype. Figure 3 displays an example of the  
348 significant SNP information from the GWAS results. Accordingly, three key features are present  
349 including variant effect prediction information, external links about the variant, and the related  
350 literature. PGSbuilder uses ClinVar<sup>41</sup> and VEP<sup>28</sup> for variant interpretation (Fig. 3B). Several  
351 external links are provided to easily navigate the further variant information (Fig. 3C). Lastly,  
352 PGSbuilder integrates the literature mining results from the pubmedKB<sup>29</sup> to assist researchers  
353 and clinical professionals in obtaining the related literature.

354

### 355 System performance

356 For benchmarking, we recorded execution time, average memory, and CPU usage for QC,  
357 GWAS, and PRS methods with 680k SNPs given 20k, 50k, and 110k samples (Table 1). The  
358 resource for each execution was limited to 20 GB and 10 CPUs. Obviously, more resources were  
359 needed as the sample size increased. Table 1 shows the comparison between six PRS methods.  
360 PRSice2, PRS-CS, and GenEpi took much more execution time than the others, but PRSice2 and  
361 GenEpi used the least CPU and memory respectively. In conclusion, it takes about three days to  
362 complete a comprehensive PRS analysis for a dataset with 110k samples and 680k SNP.

363

364

365 **Table 1.** The system performance, including execution time, average CPU, and memory of PGSbuilder.  
366 We performed QC, GWAS, and six PRS methods (classification for a binary trait) on a dataset with the  
367 same number of SNPs but different sample sizes.

Sample	STATS	QC	GWAS	C+T	Lassosum	LDpred2	PRSice2	PRS-CS	GenEpi	Total
20k	Time (min)	8.0	8.0	15.5	18.8	27.3	79.2	171.8	450.9	779.5
20k	Avg. CPU	2.9	6.9	5.6	4.7	6.3	3.3	7.5	7.7	
20k	Memory (GB)	5.1	2.0	10.9	10.5	10.9	10.7	8.4	3.8	
50k	Time (min)	43.5	20.0	33.4	41.6	73.9	180.8	268.6	715.0	1376.8
50k	Avg. CPU	4.7	6.8	7.9	7.6	7.6	5.6	8.0	7.4	
50k	Memory (GB)	16.0	1.7	16.2	16.1	15.8	14.8	12.9	3.8	
110k	Time (min)	139.5	77.0	200.3	220.3	251.3	510.6	967.3	2086.9	4453.1
110k	Avg. CPU	4.8	8.6	7.4	7.3	7.6	5.5	8.0	7.2	
110k	Memory (GB)	19.4	13.8	17.0	17.0	16.7	13.9	12.0	10.6	

368  
369 **Case Study**  
370 To demonstrate the capability of PGSbuilder, we performed two case studies using the cohorts  
371 with a large number of individuals and corresponding phenotypes. Firstly, in the Taiwan  
372 Biobank (TWB)<sup>37</sup>, a Taiwanese cohort composed of healthy adults, we previously defined nine  
373 quantitative traits and five binary traits related to some common chronic diseases, such as type 2  
374 diabetes or dyslipidemia, according to their phenotypic measures (see  
375 <https://github.com/chienyuchen/TWB-PRS> for more information). The presented GWAS and  
376 PRS models across fourteen traits in the TWB were built by using PGSbuilder. Among them,  
377 low-density lipoprotein (LDL), a quantitative trait, was selected here to demonstrate the usage of

378 adding covariates and the leverage of external summary statistics to run PGSbuilder. Secondly,  
379 for the cohort with a specific disease, we performed GWAS and PRS analysis on the National  
380 Institute on Aging (NIA)-funded Alzheimer Disease Centers (ADC) Cohort<sup>40</sup> to demonstrate the  
381 result of a binary trait.

382

383 *Low-density lipoprotein:* Low-density lipoprotein (LDL), which is a kind of lipoprotein to  
384 transport fat molecules around the body, acts as the primary driver of atherogenesis resulting in  
385 cardiovascular diseases<sup>42</sup>. Several genes, such as LDLR, PCSK9, and APOB, affecting the  
386 quantity of LDL in circulation have been reported<sup>43</sup>. Recognizing people with a genetic tendency  
387 for high LDL could help them by providing early intervention to avoid the progression of severe  
388 cardiovascular diseases. Therefore, in this study, we applied GWAS and PRS analysis using  
389 PGSbuilder on the TWB data. The covariates, including age, sex, and body mass index (BMI),  
390 were added to correct GWAS for genetic factors and then serve as clinical factors to build  
391 regression models for risk prediction.

392

393 With the default QC settings of PGSbuilder, 55,412 samples and 276,068 SNPs were passed the  
394 quality control (Table S1-2). To control the population stratification, PGSbuilder always  
395 performs PCA analysis and applies the top ten principal components (PCs) as covariates during  
396 GWAS. Figure 4A demonstrates the distribution of PC1 and PC2 to confirm SNPs without  
397 unusual differentiation between quantiles in the TWB data. The interactive Manhattan plot is  
398 shown in Figure 4B and the significant SNPs with a *P*-value  $< 10^{-5}$  are highlighted in orange for  
399 clicking to navigate variant information. Notably, in comparison with the previous study using  
400 the same TWB data<sup>44</sup>, highly similar results were observed in PGSbuilder as shown that more  
401 than 80% (89/111) of significant SNPs in the TWB arrays were identically found to associate  
402 with the LDL trait. That is, the pipeline in PGSbuilder is indeed reproducible.

403

404 In addition, PGSbuilder allows users to provide external summary statistics to build PRS models.  
405 Herein, the external summary statistics from the BioBank Japan<sup>45</sup> to identify significant variants  
406 and stratify people by the risk of high LDL were applied to estimate PRS in the TWB data.  
407 Figure 4C shows the performance on the test set of each PRS method with and without clinical  
408 factors. Overall, PRS combined with clinical factors performs better than PRS-only and clinical

409 factors-only models. These results indicate that the genetic factor combined with clinical factors  
410 provide a better prediction effect. Figure 4D depicts the risk stratification of models using  
411 clinical factors. “PRS + clinical factors” models stratified the test set better than the “clinical  
412 factors-only” model. In the “PRS + clinical factors” models, the difference in average LDL  
413 between the first and last groups is up to forty. Furthermore, the weight of each feature in the  
414 “PRS-clinical factors” model is listed in Table 2, where PRS has the largest contribution in all  
415 the models.

416

417 **Table 2.** The weight of PRS and clinical factors for “PRS + clinical factors” models of LDL.

	<b>C+T</b>	<b>PRSiце2</b>	<b>Lassosum</b>	<b>LDpred2</b>	<b>PRS-CS</b>
<b>PRS</b>	7.96	7.93	8.70	5.29	5.87
<b>Sex</b>	2.57	2.57	2.64	2.55	2.53
<b>Age</b>	4.29	4.29	4.26	4.31	4.29
<b>BMI</b>	4.41	4.41	4.45	4.33	4.34

418

419 *Alzheimer’s disease:* Alzheimer’s disease (AD), the major cause of dementia, is a complex  
420 disorder associated with genetic factors and environmental factors<sup>46</sup>. Several genetic loci, such as  
421 APOE, have been identified at the level of association study<sup>47,48</sup>. Combining the effects of these  
422 genetic loci to build a PRS model could provide individuals with the disease risk for further  
423 preventive strategies<sup>49</sup>. In this study, to build PRS models based on different methods and  
424 compare the performance of them, we analyzed the National Institute on Aging (NIA)-funded  
425 Alzheimer Disease Centers (ADC) cohort using PGsbuilder.

426

427 Figure 5 shows the performance of PRS analysis from PGsbuilder. There are two obvious  
428 groups with different performances. C+T, PRSiце2, Lassosum, and GenEpi have better auROC  
429 than LDpred2 and PRS-CS (Figure 5A). Figure 5B depicts the prediction distribution of cases  
430 and controls; the more distance between the distributions the better performance of the model.  
431 For further comparison of different methods, an UpSet plot depicts the intersection of top-100  
432 valuable SNPs from each method (Figure 5C). Notably, LDpred2 and PRS-CS have some

433 distinct SNPs than others, which might cause noise for the PRS prediction and decrease the  
434 model performance.

435

436 To investigate the information of SNPs, PGSbuilder annotates SNPs using VEP<sup>28</sup> and  
437 pubmedKB<sup>29</sup>. For example, Figure 5D shows the annotation of rs157580, which is an intron  
438 variant of gene TOMM40 with average allele frequency across different populations. A previous  
439 study (PMID: 21867541) also reported that rs157580 was significantly associated with AD<sup>50</sup>.  
440 The literature mining of PubMed abstracts by pubmedKB facilitates users to interpret the  
441 variants more readily.

442

443

## 444 **Discussion**

445 PGSbuilder is a cloud-based platform that offers comprehensive genotyping analyses, including  
446 GWAS and PRS, all in one place. Our goal for GWAS is to help identify significant SNPs  
447 associated with the target phenotype, while for PRS, we aim to assist evaluation of the prediction  
448 performance of polygenic models. Customized settings are available for users to adjust the  
449 analytic process, such as quality control, population stratification, and the selection of PRS  
450 methods. With PGSbuilder's interactive interfaces, users can easily interpret their results. For  
451 instance, users can select specific SNPs on the Manhattan plot and view the corresponding  
452 annotations in the table. Additionally, PGSbuilder integrates pubmedKB for variant  
453 interpretation by providing literature support. With these features, PGSbuilder is a  
454 comprehensive and user-friendly platform for GWAS and PRS.

455

456 In addition to the analytic pipeline, PGSbuilder offers various visualization plots to compare the  
457 performance of different PRS methods. To evaluate risk stratification, the quantile plot is a key  
458 interpretation tool. The UpSet plot enables users to observe the intersection of important SNPs  
459 selected from each method. Additionally, PGSbuilder incorporates our original GenEpi  
460 software<sup>36</sup>, which provides a unique method to uncover the genetic epistasis associated with  
461 phenotypes, as demonstrated in other recent studies<sup>51,52</sup>. Finally, as clinical factors are provided,  
462 PGSbuilder will rank the weights of them and PRS to highlight the most predictive feature,  
463 which helps users investigate the risk factor precisely.

464

465 While PGSbuilder provides a range of useful features, there are some limitations to its  
466 functionality. First, it is important to consider the limitations of hardware resources when dealing  
467 with large datasets. For example, some imputed files containing 10 million SNPs and 50K  
468 samples may not be immediately accessible due to these restrictions. However, computationally  
469 efficient methods such as C+T, Lassosum, and PRSice2 can be effectively applied to such  
470 datasets, based on our internal experiments. It is worth noting that building a predictive model  
471 using some PRS methods may require a significant amount of time. On the other hand, GenEpi,  
472 which discovers the gene-based epistasis, is not practical for imputed data due to its  
473 computational complexity. Secondly, some known PRS methods, such as those based on a  
474 mixture model for SNP effective size (e.g. SBayesR<sup>14</sup>, DPR<sup>53</sup>, DBSLMM<sup>54</sup>), are currently not  
475 included in PGSbuilder. Lastly, PRS models can only be downloaded from PGSbuilder output  
476 directly. Going forward, we are planning to implement a prediction module that allows users to  
477 upload other datasets and then automatically obtain predictions of available PRS models .

478

479 The field of PRS development is growing rapidly, with mounting evidence using the wealth of  
480 data collected in biobanks<sup>55-58</sup>. As the proof of concept is solidly demonstrated, an effective and  
481 comprehensive platform is necessary to perform GWAS and PRS analysis for diseases that are  
482 not covered by biobanks. PGSbuilder provides researchers with the ability to identify significant  
483 loci with annotations and investigate the polygenicity of a target phenotype across a specific  
484 population effectively. By leveraging genotypes, a PRS model has the clinical potential to offer  
485 risk evaluations to individuals. This, in turn, can facilitate early surveillance for severe diseases.

486

487

## 488 Conclusion

489 PGSbuilder is an end-to-end platform that seamlessly integrates QC of genotype data, GWAS,  
490 PRS, SNP annotation, and visualizations. This platform is versatile, allowing the incorporation of  
491 external GWAS summary statistics to run PRS using various methods, thereby enabling the  
492 estimation of genetic risk in smaller cohort samples. In addition, PGSbuilder's user-friendly  
493 interface is designed to be accessible to users without programming experiences. In the future,

494 we plan to further augment and broaden PGSbuilder by introducing a prediction module that  
495 allows users to directly run their PRS models for specific disease phenotypes.

496

497

## 498 **Acknowledgements**

499 We thank Tzu-Hung Hsiao and Chien-Lin Mao for valuable early discussion and pipeline testing.

500

501

## 502 **Funding**

503 This work was supported by the Ministry of Science and Technology, Taiwan (MOST 109-2221-  
504 E-002-161-MY3 and MOST 109-2221-E-002 -162 -MY3).

505

506

## 507 **Data and software availability**

508 All genetic and phenotype data in TWB described in this paper are publicly available via the  
509 Taiwan Biobank data access protocol. Fourteen PRS models using TWB data, including five  
510 binary phenotypes and nine quantitative traits, are freely available on the GitHub project  
511 repository (<https://github.com/chienyuchen/TWB-PRS>). The AD data is publicly available to  
512 registered researchers by request from the National Institute on Aging Genetics of Alzheimer's  
513 Disease Data Storage Site (NIAGADS). The source codes for GWAS and PRS analyses were  
514 deposited to Github and is available at <https://github.com/ailabstw/PGSbuilder>.

515

## 516 **Ethics approval and consent to participate**

517 The application number of TWB data is TWBR10411-03. This application of NIA ADC Cohort  
518 dataset has been filed with the IRB ( 202106049RINA) in order to get approval from NIAGADS.

519

520

## 521 **Competing interests**

522 The authors declare that they have no competing interests.

523

524

525 **Authors' contributions**

526 KHL, YLL, TTH, YCC, and HCC conceived and implemented the pipeline development. YCC  
527 inspired team members to unite as a product manager, and designed all the frameworks of this  
528 web service, including wireframe, prototype, and database schema. SSW, WCL, and GZF  
529 implemented the web design and interface. TFC and PHL implemented the literature mining.  
530 YLK served as liaisons to user communities. YCC and JHH helped project development and  
531 management. PLC led the application of TWB data. HFJ, HKT, CYC, and JHH supervised the  
532 project. KHL and JHH led the writing of the manuscript. All authors discussed the results and  
533 implications and commented on the manuscript. All authors read and approved the final  
534 manuscript.

535

536

537 **References**

- 538 1. Mills, M. C. & Rahal, C. A scientometric review of genome-wide association studies. *Commun Biol*  
539 **2**, 9 (2019).
- 540 2. Buniello, A. *et al.* The NHGRI-EBI GWAS Catalog of published genome-wide association studies,  
541 targeted arrays and summary statistics 2019. *Nucleic Acids Research* vol. 47 D1005–D1012 Preprint  
542 at <https://doi.org/10.1093/nar/gky1120> (2019).
- 543 3. Visscher, P. M. *et al.* 10 Years of GWAS Discovery: Biology, Function, and Translation. *Am. J.*  
544 *Hum. Genet.* **101**, 5–22 (2017).
- 545 4. Stranger, B. E., Stahl, E. A. & Raj, T. Progress and promise of genome-wide association studies for  
546 human complex trait genetics. *Genetics* **187**, 367–383 (2011).
- 547 5. Watanabe, K. *et al.* A global overview of pleiotropy and genetic architecture in complex traits. *Nat.*  
548 *Genet.* **51**, 1339–1348 (2019).
- 549 6. Chatterjee, N., Shi, J. & García-Closas, M. Developing and evaluating polygenic risk prediction  
550 models for stratified disease prevention. *Nat. Rev. Genet.* **17**, 392–406 (2016).
- 551 7. Wray, N. R. *et al.* From Basic Science to Clinical Application of Polygenic Risk Scores: A Primer.

552        *JAMA Psychiatry* **78**, 101–109 (2021).

553        8. Ma, Y. & Zhou, X. Genetic prediction of complex traits with polygenic scores: a statistical review.

554        *Trends Genet.* **37**, 995–1011 (2021).

555        9. Wray, N. R., Goddard, M. E. & Visscher, P. M. Prediction of individual genetic risk to disease from

556        genome-wide association studies. *Genome Res.* **17**, 1520–1528 (2007).

557        10. International Schizophrenia Consortium *et al.* Common polygenic variation contributes to risk of

558        schizophrenia and bipolar disorder. *Nature* **460**, 748–752 (2009).

559        11. Vilhjálmsson, B. J. *et al.* Modeling Linkage Disequilibrium Increases Accuracy of Polygenic Risk

560        Scores. *Am. J. Hum. Genet.* **97**, 576–592 (2015).

561        12. Privé, F., Arbel, J. & Vilhjálmsson, B. J. LDpred2: better, faster, stronger. *Bioinformatics* (2020)

562        doi:10.1093/bioinformatics/btaa1029.

563        13. Ge, T., Chen, C.-Y., Ni, Y., Feng, Y.-C. A. & Smoller, J. W. Polygenic prediction via Bayesian

564        regression and continuous shrinkage priors. *Nat. Commun.* **10**, 1776 (2019).

565        14. Lloyd-Jones, L. R. *et al.* Improved polygenic prediction by Bayesian multiple regression on

566        summary statistics. *Nat. Commun.* **10**, 5086 (2019).

567        15. Zhou, G. & Zhao, H. A fast and robust Bayesian nonparametric method for prediction of complex

568        traits using summary statistics. *PLoS Genet.* **17**, e1009697 (2021).

569        16. Mak, T. S. H., Porsch, R. M., Choi, S. W., Zhou, X. & Sham, P. C. Polygenic scores via penalized

570        regression on summary statistics. *Genet. Epidemiol.* **41**, 469–480 (2017).

571        17. Choi, S. W. & O'Reilly, P. F. PRSice-2: Polygenic Risk Score software for biobank-scale data.

572        *Gigascience* **8**, (2019).

573        18. Ni, G. *et al.* A Comparison of Ten Polygenic Score Methods for Psychiatric Disorders Applied

574        Across Multiple Cohorts. *Biol. Psychiatry* **90**, 611–620 (2021).

575        19. Pain, O. *et al.* Evaluation of polygenic prediction methodology within a reference-standardized

576        framework. *PLoS Genet.* **17**, e1009021 (2021).

577        20. Collister, J. A., Liu, X. & Clifton, L. Calculating Polygenic Risk Scores (PRS) in UK Biobank: A

578        Practical Guide for Epidemiologists. *Front. Genet.* **13**, 818574 (2022).

579        21. Choi, S. W., Mak, T. S.-H. & O'Reilly, P. F. Tutorial: a guide to performing polygenic risk score  
580        analyses. *Nat. Protoc.* **15**, 2759–2772 (2020).

581        22. Wray, N. R. *et al.* Research review: Polygenic methods and their application to psychiatric traits. *J.*  
582        *Child Psychol. Psychiatry* **55**, 1068–1087 (2014).

583        23. Lambert, S. A. *et al.* The Polygenic Score Catalog as an open database for reproducibility and  
584        systematic evaluation. *Nat. Genet.* **53**, 420–425 (2021).

585        24. Martin, A. R. *et al.* Clinical use of current polygenic risk scores may exacerbate health disparities.  
586        *Nat. Genet.* **51**, 584–591 (2019).

587        25. Scutari, M., Mackay, I. & Balding, D. Using Genetic Distance to Infer the Accuracy of Genomic  
588        Prediction. *PLoS Genet.* **12**, e1006288 (2016).

589        26. Wang, Y. *et al.* Theoretical and empirical quantification of the accuracy of polygenic scores in  
590        ancestry divergent populations. *Nat. Commun.* **11**, 3865 (2020).

591        27. Folkersen, L. *et al.* Impute.me: An Open-Source, Non-profit Tool for Using Data From Direct-to-  
592        Consumer Genetic Testing to Calculate and Interpret Polygenic Risk Scores. *Front. Genet.* **11**, 578  
593        (2020).

594        28. McLaren, W. *et al.* The Ensembl Variant Effect Predictor. *Genome Biol.* **17**, 122 (2016).

595        29. Li, P.-H. *et al.* pubmedKB: an interactive web server for exploring biomedical entity relations in the  
596        biomedical literature. *Nucleic Acids Res.* (2022) doi:10.1093/nar/gkac310.

597        30. Chang, C. C. *et al.* Second-generation PLINK: rising to the challenge of larger and richer datasets.  
598        *Gigascience* **4**, 7 (2015).

599        31. Manichaikul, A. *et al.* Robust relationship inference in genome-wide association studies.  
600        *Bioinformatics* **26**, 2867–2873 (2010).

601        32. Consortium, T. I. H. 3. & The International HapMap 3 Consortium. Integrating common and rare  
602        genetic variation in diverse human populations. *Nature* vol. 467 52–58 Preprint at  
603        <https://doi.org/10.1038/nature09298> (2010).

604 33. Marees, A. T. *et al.* A tutorial on conducting genome-wide association studies: Quality control and  
605 statistical analysis. *International Journal of Methods in Psychiatric Research* **27**, e1608 (2018).

606 34. Price, A. L. *et al.* Principal components analysis corrects for stratification in genome-wide  
607 association studies. *Nat. Genet.* **38**, 904–909 (2006).

608 35. Purcell, S. *et al.* PLINK: a tool set for whole-genome association and population-based linkage  
609 analyses. *Am. J. Hum. Genet.* **81**, 559–575 (2007).

610 36. Chang, Y.-C. *et al.* GenEpi: gene-based epistasis discovery using machine learning. *BMC*  
611 *Bioinformatics* **21**, 68 (2020).

612 37. Feng, Y.-C. A. *et al.* Taiwan Biobank: a rich biomedical research database of the Taiwanese  
613 population. Preprint at <https://doi.org/10.1101/2021.12.21.21268159>.

614 38. Lin, Y.-H. *et al.* variant2literature: full text literature search for genetic variants. *bioRxiv* 583450  
615 (2019) doi:10.1101/583450.

616 39. Page, L., Brin, S., Motwani, R. & Winograd, T. The PageRank Citation Ranking: Bringing Order to  
617 the Web. (1999).

618 40. Naj, A. C. *et al.* Common variants at MS4A4/MS4A6E, CD2AP, CD33 and EPHA1 are associated  
619 with late-onset Alzheimer's disease. *Nat. Genet.* **43**, 436–441 (2011).

620 41. Landrum, M. J. *et al.* ClinVar: improving access to variant interpretations and supporting evidence.  
621 *Nucleic Acids Res.* **46**, D1062–D1067 (2018).

622 42. Borén, J. *et al.* Low-density lipoproteins cause atherosclerotic cardiovascular disease:  
623 pathophysiological, genetic, and therapeutic insights: a consensus statement from the European  
624 Atherosclerosis Society Consensus Panel. *Eur. Heart J.* **41**, 2313–2330 (2020).

625 43. Borén, J. *et al.* Low-density lipoproteins cause atherosclerotic cardiovascular disease:  
626 pathophysiological, genetic, and therapeutic insights: a consensus statement from the European  
627 Atherosclerosis Society Consensus Panel. *Eur. Heart J.* **41**, 2313–2330 (2020).

628 44. Chen, C.-Y. *et al.* Analysis across Taiwan Biobank, Biobank Japan and UK Biobank identifies  
629 hundreds of novel loci for 36 quantitative traits. Preprint at

630 https://doi.org/10.1101/2021.04.12.21255236.

631 45. Sakaue, S. *et al.* A cross-population atlas of genetic associations for 220 human phenotypes. *Nat. Genet.* **53**, 1415–1424 (2021).

632 46. Breijyeh, Z. & Karaman, R. Comprehensive Review on Alzheimer's Disease: Causes and Treatment. *Molecules* **25**, (2020).

633 47. Wightman, D. P. *et al.* A genome-wide association study with 1,126,563 individuals identifies new risk loci for Alzheimer's disease. *Nat. Genet.* **53**, 1276–1282 (2021).

634 48. Bellenguez, C. *et al.* New insights into the genetic etiology of Alzheimer's disease and related dementias. *Nat. Genet.* **54**, 412–436 (2022).

635 49. de Rojas, I. *et al.* Common variants in Alzheimer's disease and risk stratification by polygenic risk scores. *Nat. Commun.* **12**, 3417 (2021).

636 50. Simmons, C. R., Zou, F., Younkin, S. G. & Estus, S. Evaluation of the global association between cholesterol-associated polymorphisms and Alzheimer's disease suggests a role for rs3846662 and HMGCR splicing in disease risk. *Mol. Neurodegener.* **6**, 62 (2011).

637 51. Yashin, A. I. *et al.* Roles of interacting stress-related genes in lifespan regulation: insights for translating experimental findings to humans. *J Transl Genet Genom* **5**, 357–379 (2021).

638 52. Rodrigo, L. M. & Nyholt, D. R. Imputation and Reanalysis of ExomeChip Data Identifies Novel, Conditional and Joint Genetic Effects on Parkinson's Disease Risk. *Genes* **12**, (2021).

639 53. Zeng, P. & Zhou, X. Non-parametric genetic prediction of complex traits with latent Dirichlet process regression models. *Nat. Commun.* **8**, 456 (2017).

640 54. Yang, S. & Zhou, X. Accurate and Scalable Construction of Polygenic Scores in Large Biobank Data Sets. *Am. J. Hum. Genet.* **106**, 679–693 (2020).

641 55. Zhang, R. *et al.* Novel disease associations with schizophrenia genetic risk revealed in ~400,000 UK Biobank participants. *Mol. Psychiatry* **27**, 1448–1454 (2022).

642 56. Richardson, T. G., Harrison, S., Hemani, G. & Davey Smith, G. An atlas of polygenic risk score associations to highlight putative causal relationships across the human genome. *Elife* **8**, (2019).

656 57. Sakaue, S. *et al.* Trans-biobank analysis with 676,000 individuals elucidates the association of  
657 polygenic risk scores of complex traits with human lifespan. *Nat. Med.* **26**, 542–548 (2020).

658 58. Shen, X. *et al.* A genome-wide association and Mendelian Randomisation study of polygenic risk  
659 for depression in UK Biobank. *Nat. Commun.* **11**, 2301 (2020).

660 59. Sherry, S. T. dbSNP: the NCBI database of genetic variation. *Nucleic Acids Research* vol. 29 308–  
661 311 Preprint at <https://doi.org/10.1093/nar/29.1.308> (2001).

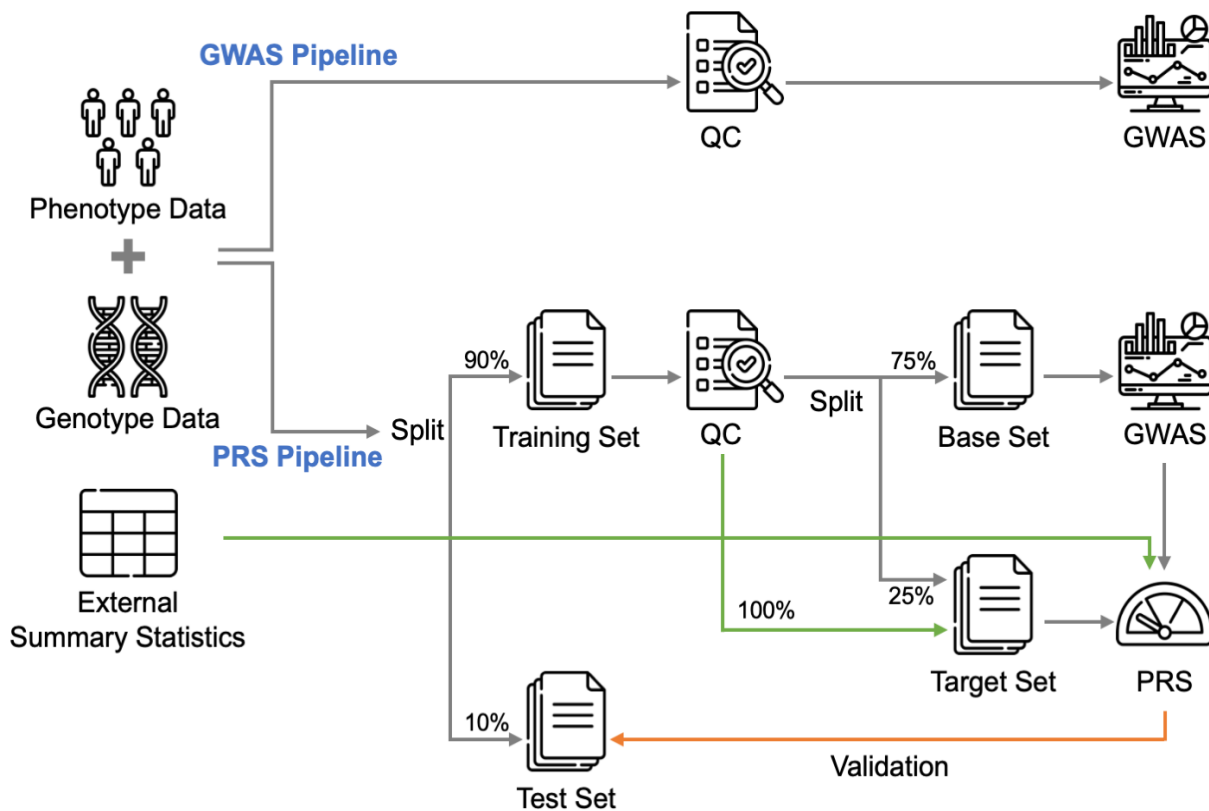
662 60. Karczewski, K. J. *et al.* The mutational constraint spectrum quantified from variation in 141,456  
663 humans. *Nature* **581**, 434–443 (2020).

664 61. Safran, M. *et al.* The GeneCards Suite. in *Practical Guide to Life Science Databases* (eds.  
665 Abugessaisa, I. & Kasukawa, T.) 27–56 (Springer Nature Singapore, 2021).

666 62. Lex, A., Gehlenborg, N., Strobelt, H., Vuillemot, R. & Pfister, H. UpSet: Visualization of  
667 Intersecting Sets. *IEEE Trans. Vis. Comput. Graph.* **20**, 1983–1992 (2014).

668 **Figures and Figure legends**

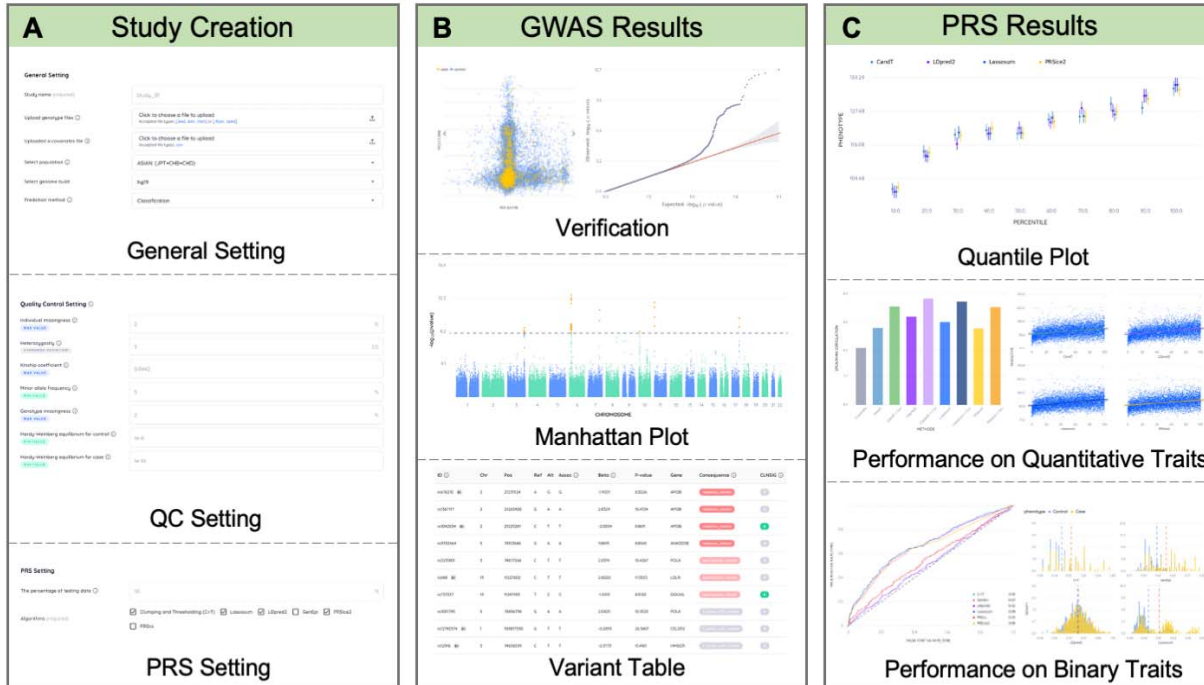
669



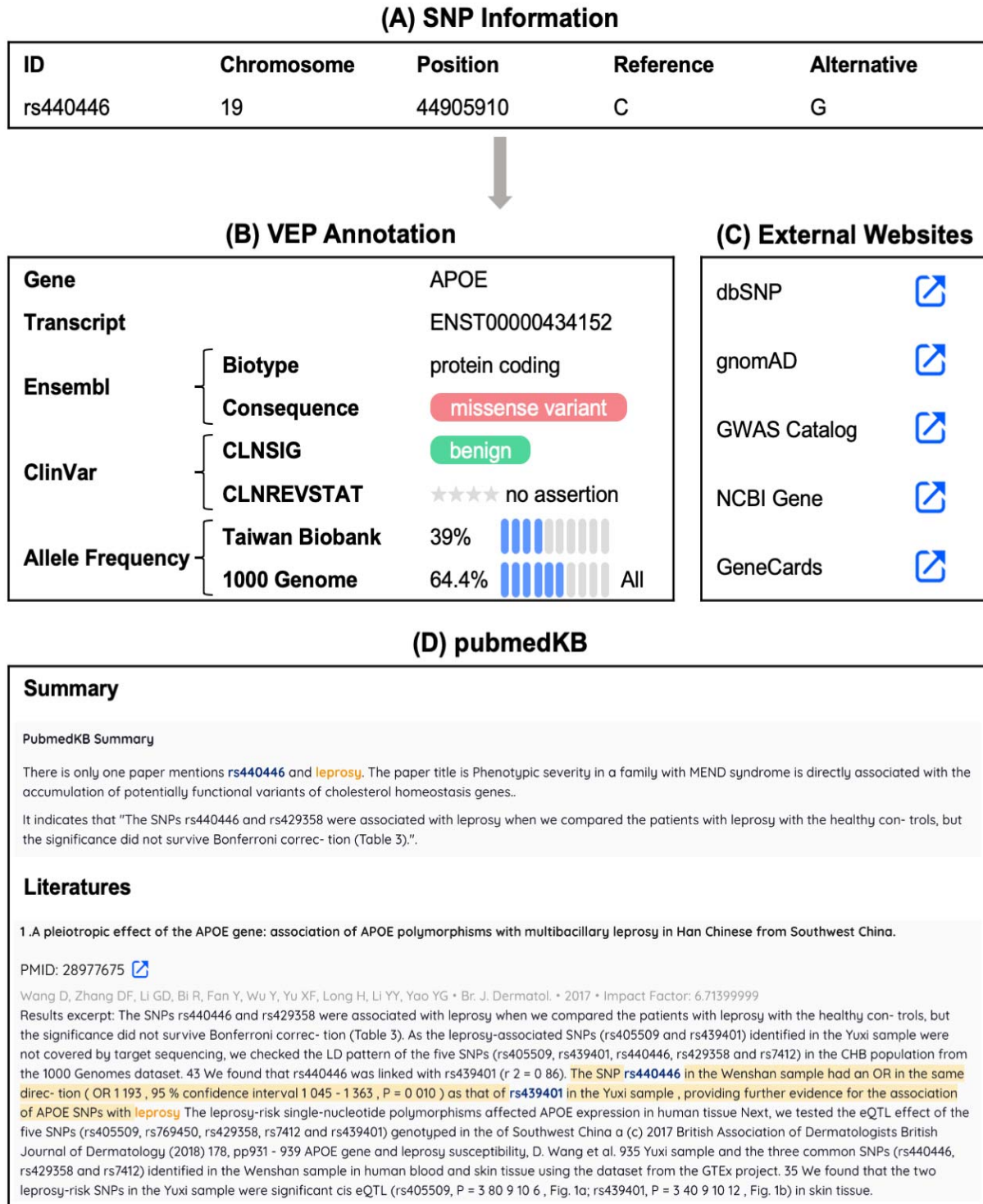
670

671 **Figure 1. Analysis pipelines of PGSbuilder.** PGSbuilder performs GWAS and PRS analysis  
672 respectively on the input dataset. For the GWAS pipeline, PGSbuilder applies QC followed by  
673 GWAS on the whole input dataset. For the PRS pipeline, PGSbuilder splits the input dataset into  
674 training and test sets with the default ratio of 9:1 and applies QC on the training set. The training  
675 set is later split into base and target subsets with a ratio of 3:1, and the GWAS result is obtained  
676 from the base set. Combining the target set with the summary statistics derived from the base set,  
677 PGSbuilder builds PRS models based on different PRS methods. Alternatively, users could  
678 provide external summary statistics and the entire training set will be used to build the PRS  
679 model. Finally, the independent test set is used to evaluate the performance of the PRS model.

680



681  
682 **Figure 2. PGsbuilder interface and visualizations.** (A) First of all, users can create a new  
683 study with customization, including general, QC, and PRS settings. (B) After analysis, GWAS  
684 results are composed of verification, including the PCA and Q-Q plots, and significant SNPs,  
685 including the Manhattan plot and variant table. (C) On the other hand, PRS results show a  
686 quantile plot for risk stratification and performance comparison for quantitative or binary traits.

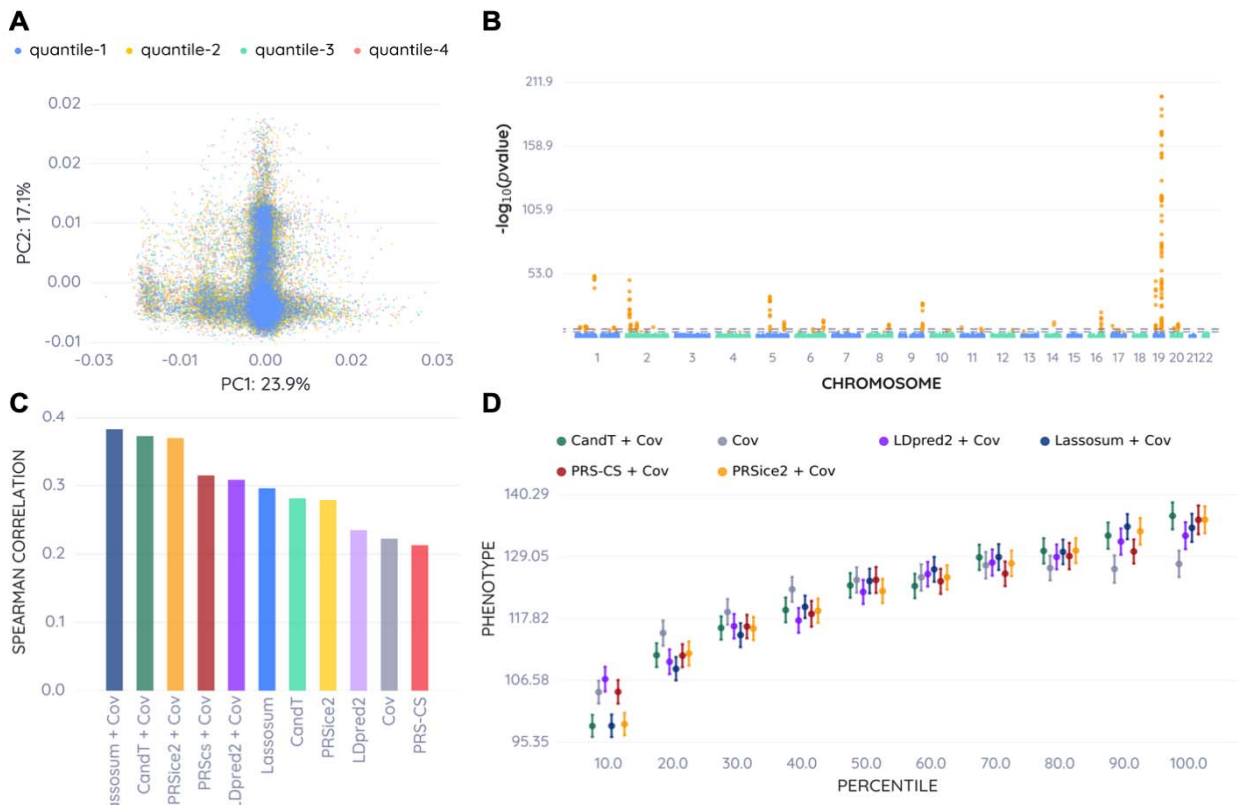


688

689 **Figure 3. Example annotation result of SNP “rs440446” on PGStbuilder.** (A) There is the  
 690 basic information and statistics (e.g. GWAS  $P$ -value) of the variant. (B) We apply different  
 691 colors on consequence (the red one) and ClinVar significance (the green one) according to tables

692 provided by Ensembl and ClinVar, respectively, for a better presentation of SNP importance  
693 level. The following block is the transcript ID, ClinVar significance, and allele frequency from  
694 VEP. (C) We also provided links to external websites with more variant or gene information,  
695 such as dbSNP<sup>59</sup>, gnomAD<sup>60</sup>, GWAS Catalog<sup>2</sup>, and GeneCards<sup>61</sup>. (D) The block at the bottom is  
696 the results from pubmedKB. The summary presents the sentence where the SNP and the  
697 phenotype co-occur, and we show the paper snippet of odds ratio statistics.

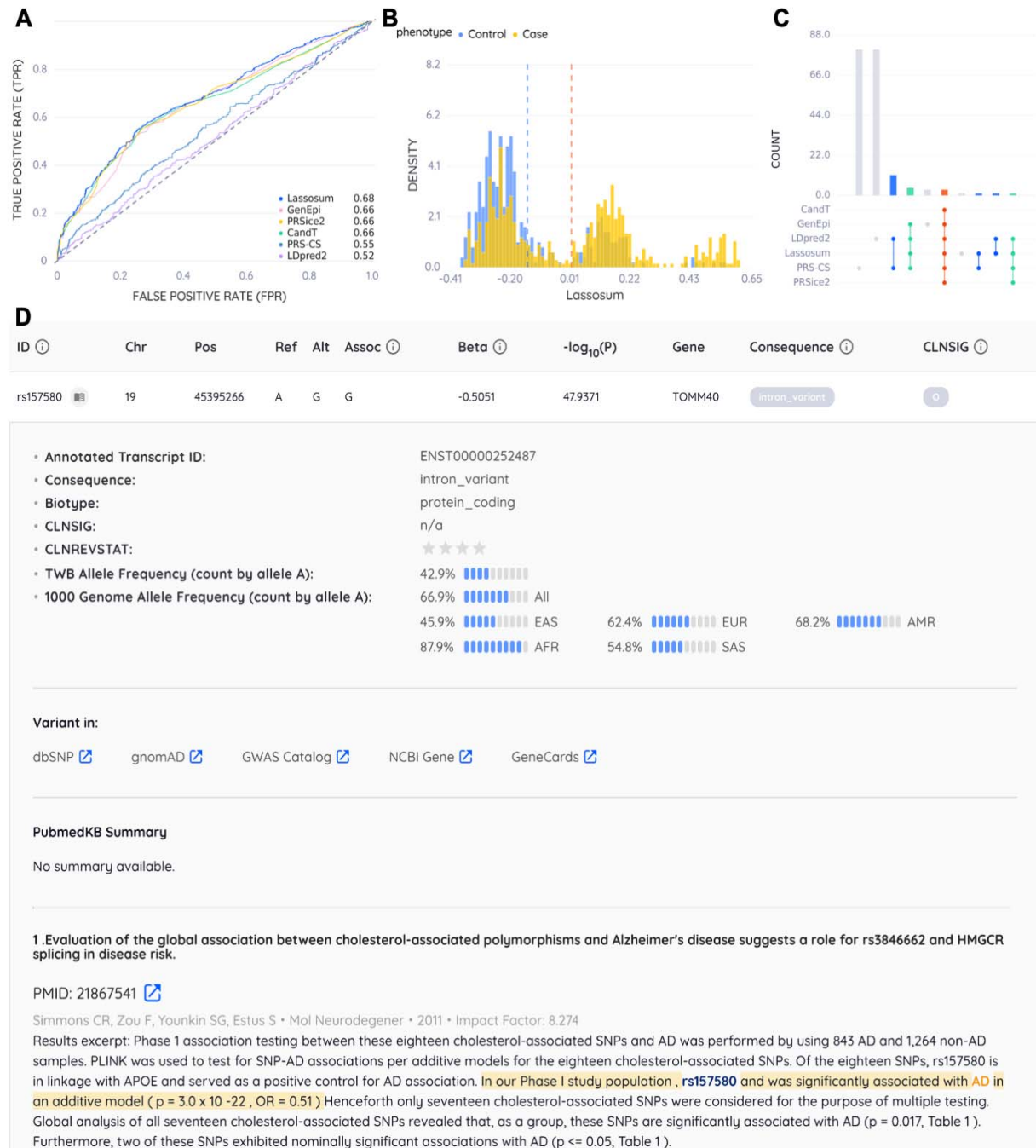
698



699

700 **Figure 4. Results of LDL GWAS and PRS analyses.** (A) PCA plot of the first and second PCs.  
701 To view any deviation of PCs among the samples, values of the quantitative phenotype are  
702 separated into four quantiles. (B) Manhattan plot of  $-\log_{10}(P\text{-value})$ . GWAS is performed on  
703 autosomal SNPs, and SNPs with  $P\text{-value} < 10^{-5}$  are colored in orange. (Source data in Table S3)  
704 (C) Bar plot of Spearman's correlation of each PRS model. Models derived from different  
705 methods with or without covariates (Cov) are demonstrated simultaneously. (Source data in  
706 Table S4) (D) Quantile plot for risk stratification. The “covariate-only (Cov)” model and “PRS  
707 + covariate” models are plotted to compare the usage of genetic factors. (Source data in Table  
708 S5).

709



710

711 **Figure 5. Results of AD across different PRS methods.** (A) ROC curve of each PRS model on  
712 the test set. (Source data in Table S6) (B) Prediction distributions of the Lassosum PRS model  
713 for cases (yellow) and controls (blue). The dashed line represents the mean of each group. (C)  
714 UpSet plot<sup>62</sup> for the intersection of important SNPs derived from different PRS methods. The  
715 intersection, or the combination, of methods are presented as the matrix layout while the variant  
716 counts of each intersection are shown as the histogram. Different colors represent the number of

717 PRS methods. (corresponding output data in Table S7) (D) Annotations for SNP “rs157580”. On  
718 the top is the basic information and statistics of the variant. The following block is the transcript  
719 ID, ClinVar significance and allele frequency from VEP<sup>28</sup>. In addition, we also provided links to  
720 external websites with more variant information, such as dbSNP<sup>59</sup> and gnomAD<sup>60</sup>. The block in  
721 the bottom is the results from pubmedKB<sup>29</sup> which highlights the odds ratio of AD in the presence  
722 of this variant.